Dispersion of Carbon Nanotubes in Organic Solvents Initiated by Hydrogen Bonding Interactions

Lili Li, Wei Feng, and Peijun Ji
Dept. of Biochemical Engineering, Dept. of Chemical Engineering, Beijing University of Chemical Technology, Beijing, 100029, China

DOI 10.1002/aic.13724
Published online January 17, 2012 in Wiley Online Library (wileyonlinelibrary.com).

Phase transfer of multiwalled carbon nanotubes (MWNTs) from an aqueous phase into an organic phase is achieved. The transfer uses the hydrogen-bonding interactions between the disaccharide group of a sugar-based amphiphile and oxygenated functional groups on the surface of MWNTs. The dispersion of carbon nanotubes in a wide range of organic solvents is enabled, which represents the first example of solubilization of carbon nanotubes in organic solvents via hydrogen bonding interactions. © 2012 American Institute of Chemical Engineers *AIChE J,* 58: 2997–3002, 2012
Keywords: phase transfer, sugar-based amphiphile, absorption, separations, solutions, selectivity

Introduction

Carbon nanotubes (CNTs) possess superior electrical, mechanical, optical, thermal, and chemical properties and have many promising applications.[1–5] Dispersions of CNTs in organic solvents are the basis for medium-tech applications.[6,7] Their solubility/dispersibility is important for a ready manipulation and a feasible solution-phase processing of CNTs into devices,[7] and for using carbon nanotubes within widespread applications.[8]

Some functionalization methods are used to enhance dispersion of CNTs in organic solvents. CNTs in amide form are dispersed in chloroform, benzene, toluene, or other organic solvents.[9–11] Dichlorocarbene- functionalized CNTs,[12] nanotubes derivatized with a 4-*tert*-butylbenzene moiety[13] and polymer functionalized CNTs[8,14] were found to possess improved solubility in organic solvents.

Dispersion of CNTs in organic solvents can be achieved through phase transfers, including the length-dependent transfer of CNTs from the aqueous phase to the organic phase using electrostatic interactions[15] and the phase transfer of amide functionalized CNTs.[16] Phase transfer of CNTs may have potential for applications, such as facilitating the incorporation of CNTs into polymer matrices.[17] The study of phase transfer of CNTs can benefit the study of water/oil interface phenomena. These include the fabrication of ultrathin films,[18] formation of CNT-metal nanoparticle films[19] and biocatalysis using the CNT-enzyme conjugate[20] at water/oil interfaces, the fabrication of CNT capsules using water-in-oil emulsion techniques,[21] and selective removal of CNT bundles from an aqueous dispersion via interfacial trapping.[22,23] In this work, the phase transfer of MWNTs from an aqueous phase to an organic phase with a sugar-based amphiphile *N*-hexadecyl-D-maltosylamine (HDMA) is investigated. The transfer is initiated by the hydrogen bonding interactions between the acid-oxidized MWNTs and the amphiphile.

Experiment

Materials

Multiwalled carbon nanotubes were purchased from Shenzhen Nanotech Port Co. (Shenzhen, China). The purity was higher than 95%, and the catalyst residue was less than 0.2%. D-maltose, hexadecylamine, Triton X-100, polyvinylpyrrolidone (PVP), Tween 20, hexadecyltrimethylammonium bromide (CTAB), and dioctyl sodium sulfosuccinate (AOT), and petroleum ether were purchased from Sigma-Aldrich (Shanghai, China) and were used as received. Isooctance, hexane, carbon tetrachloride, propanol, 2-propanol, ethanol, and n-butanol were obtained from Sinopharm Chemical Reagent Co.(Beijing, China), the chemicals were of analytical reagent grade and were used as supplied.

Synthesis of N-hexadecyl-D-maltosylamine (HDMA)

HDMA as shown in scheme S1 (see online for Additional Supporting Information) was synthesized according to the method as described elsewhere.[24] 3.0 mmol of D-maltose was dissolved in 6.0 mL of deionized water; 5.0 mmol of hexadecylamine was dissolved in 10.0 mL of 2-propanol. The two solutions were mixed and stirred at room temperature. When the solution turned turbid, it was heated to 60°C to dissolve the precipitate; and then the solution was stirred at room temperature. The mixture was stirred for 24 h with periodic heating to 60°C at regular intervals as and when the solution turned turbid. The crude residue was dried *in vacuo*, and then recrystallized from ethanol and then again freeze-dried to eliminate traces of water. The structure of synthesized HDMA was characterized by ^{1}H NMR (DMSO-d6, 600 MHz): 0.855 (t, 3H), 1.238 (m, 28H), δ2.175 (br s, 1H),

Additional Supporting Information can be found in the online version of this article.

Correspondence concerning this article should be addressed to W. Feng at fengwei@mail.buct.edu.cn; P. Ji at jipj@mail.buct.edu.cn.

2.501 (m, 1H), 2.771 (m, 2H), 2.908–3.684 (m, 6H), 4.310–5.429 (m, 4H).

Oxidation of MWNTs

MWNTs were purified and oxidized as reported elsewhere.[25] As-received MWNTs were purified by refluxing in an aqueous HNO_3 of 2.6 M at 70°C for 45 h. The nanotube suspension was diluted and washed with double-distilled water by filtering through a 0.8 μm polycarbonate membrane. The samples were dried at 80°C *in vacuo*. The purified MWNTs were oxidized in the mixture of HNO_3 and H_2SO_4 (3:1) for 3, 6, 8, 10, and 12 h. The suspensions of oxidized MWNTs (O-MWNTs) were diluted and washed with double-distilled water by filtering through a 0.45 μm polycarbonate membrane. The samples were dried at 80°C *in vacuo*.

Infrared spectra for O-MWNTs were collected using a Fourier transform infrared (FTIR) spectrometer (Bruker TENSOR 27) equipped with a horizontal, temperature-controlled attenuated total reflectance (ATR) with ZnSe Crystal (Pike Technology). Infrared spectra were collected using a liquid-nitrogen-cooled mercury- cadmium- telluride detector that collected 128 scans per spectrum at a resolution of 2 cm^{-1}. All spectra were corrected by a background subtraction of the ATR element spectrum. Ultrapure nitrogen gas was introduced at a controlled flow rate to purge water vapor.

The distributions of oxygen-containing carboxyl, carbonyl and hydroxyl groups on O-MWNTs were determined using X-ray photoelectron spectroscopy (XPS). XPS spectra were acquired using a Thermo VG ESCALAB250 X-ray photoelectron spectrometer, which was operated at the pressure of 2×10^{-9} Pa using Mg Ka X-ray as the excitation source. Analysis of the data was carried out with Thermo Avantage XPS software.[26] All XPS spectra were referenced to the main C 1s hydrocarbon peak at 284.9 eV binding energy. A Shirley background[27] was used in all curve-fitting.[28]

Phase transfer of O-MWNTs

A solution was prepared by dissolving HDMA (12 mmol/mL) in an organic solvent, which consisted of isooctane and n-propanol in a volume ratio of 4:1. O-MWNTs were dissolved in water (1.0 mg/mL) and placed in a vial. Then, the organic solution was added to the vial at a 4:1 volume ratio resulting in a liquid-liquid phase system. The vial is shaken vigorously by vortex-mixing for 30 s or by hand for 1 min to assist transfer across the interface. Similarly, carbon tetrachloride and mixtures of hexane/isopropyl alcohol and petroleum ether/n-butanol were used as organic phases for phase transfer of O-MWNTs.

Characterization of the organic phase

The dispersibility of O-MWNTs in the organic phase was monitored by measuring ultraviolet-visible (UV–vis) spectra, which were recorded on a Shimadzu UV2550-PC spectrophotometer.

The organic phase after the phase transfer of O-MWNTs was dried at 55°C *in vacuo* to remove isooctane and n-propanol. The dried sample was used to measure X-ray diffraction (XRD) pattern. XRD patterns were obtained with a diffractometer of X' Pert PRO MPD using a Gu anode at 40 kV, wavelength 0.154 nm. The diffractograms were operated at a scan rate of 1°/min from $2\theta = 5°$ to $2\theta = 90°$.

The dried sample of an upper organic phase was obtained similarly as above and used for thermogravimetric analysis, which was performed on a PerkinElmer Diamond thermal analysis system. Samples were analyzed at a heating rate of 10°C/min to 800°C in an atmosphere of air.

HRTEM images were obtained by using a JEOL JEM-3010 F transmission electron microscope operating at 300 kV.

Results and Discussion

The phase transfers are shown in Figure 1. In vials A, B, C, D, and E, the carbon nanotubes with different oxidation time of 3 h, 6 h, 8 h, 10 h, and 12 h, respectively, were used for phase transfer. Figure 1a shows that there is no transfer of nanotubes in vial A; not all nanotubes are transferred into the organic phase in vial B, as some nanotubes (ca. 15%) are retained in the aqueous phase; and in vials C, D, and E, the amount of O-MWNTs remaining in the aqueous phase can be negligible, indicating that all nanotubes are transferred into the organic phase. The dispersibility of O-MWNTs in the organic phase was investigated by measuring UV−vis spectra. A higher UV−vis absorbance means a larger dispersibility of the O-MWNTs. Figure1b shows that the absorbance intensity of ultraviolet-visible (UV–vis) spectra increases from vial B to vial E, indicating an increased concentration of O-MWNTs in the organic phase with oxidation time. For vials C, D, and E, the intensity difference is due to some nanotubes settling at the interface between the immiscible fluids. In addition, pristine and purified MWNTs

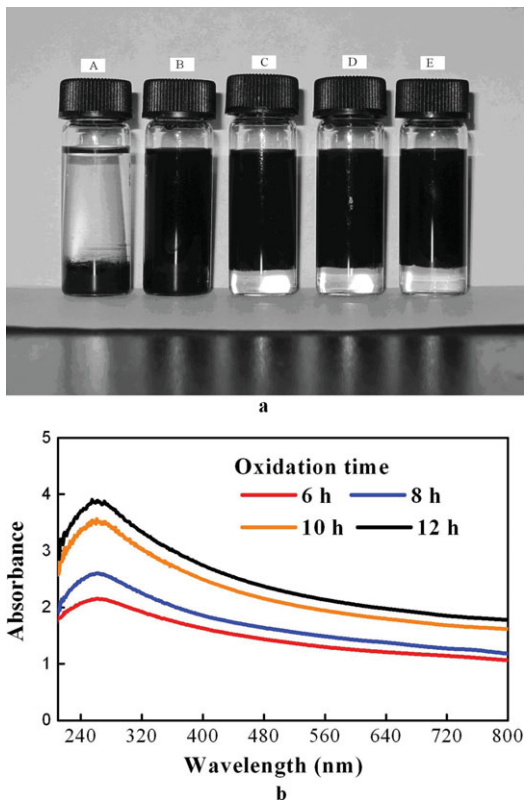

Figure 1. (a) The effect of oxidation time on the transfer of O-MWNTs into an organic phase, and (b) UV–vis spectra for the upper organic phase.

Oxidation time for carbon nanotubes: (A) 3 h; (B) 6 h; (C) 8 h; (D) 10 h; (E) 12 h. [Color figure can be viewed in the online issue, which is available at wileyonlinelibrary.com.]

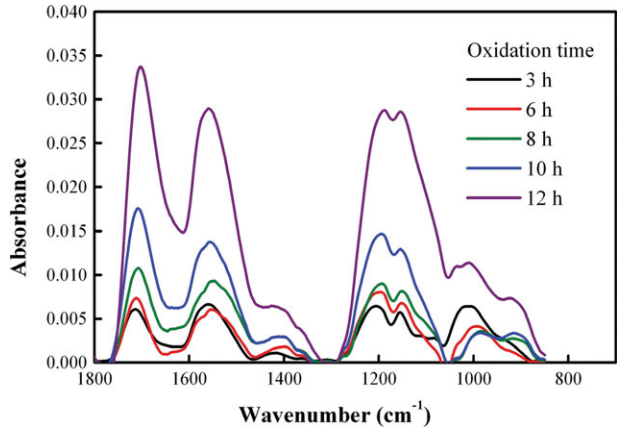

Figure 2. FTIR spectra for oxidized MWNTs with different oxidation time.

[Color figure can be viewed in the online issue, which is available at wileyonlinelibrary.com.]

could not be transferred into the organic phase with HDMA (Figures not shown). It is expected that the phase transfer is initiated by the hydrogen bonding interactions between the disaccharide head of HDMA and the functional groups on oxidized MWNTs (O-MWNTs), including carboxyl, carbonyl and hydroxyl, which are generated by the oxidation in the mixture of HNO_3 and H_2SO_4.[29] With a longer oxidation time, more oxygen groups can be produced on carbon nanotubes as illustrated by Figures 2 and 3. However, more sugar-based amphiphile molecules can interact with O-MWNTs. As a result, more O-MWNTs can be dispersed in the organic phase (Figure 1b).

The FTIR spectra of O-MWNTs clearly show the presence of oxygen-containing groups resulting from the oxidation (Figure 2). A band at 1,703 cm^{-1} is attributed to C=O stretching vibrations in carboxyl and carbonyl groups; a band around 1,185 cm^{-1} is associated with C—O stretching vibrations.[30] The C1 s XPS spectra of the oxidized MWNTs (Figure 3) suggest that oxygen atoms are bound to surface

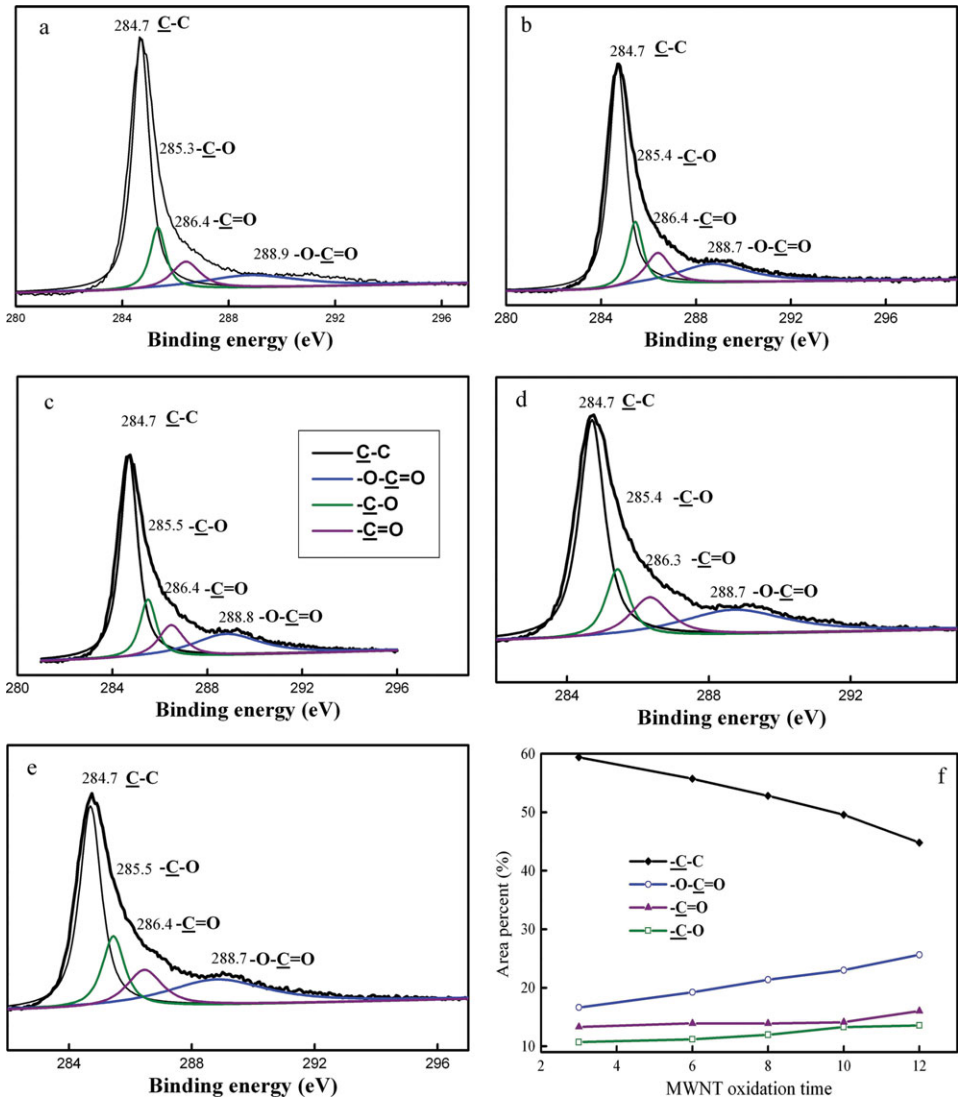

Figure 3. C1 s XPS spectra of oxidized MWNTs.

Oxidation time: (a) 3 h; (b) 6 h; (c) 8 h; (d) 10 h; (e) 12 h. [Color figure can be viewed in the online issue, which is available at wileyonlinelibrary.com.]

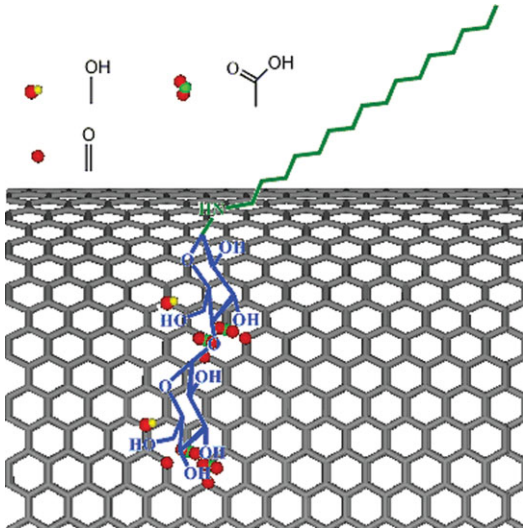

Figure 4. Schematic presentation of hydrogen bonding interactions between the disaccharide group of HDMA and the oxygen groups of the O-MWNT.

The oxygen groups are indicated by the colored circles. [Color figure can be viewed in the online issue, which is available at wileyonlinelibrary.com.]

carbon mainly through C—OH (285.4 eV), C=O (286.4 eV) and O—C=O (288.8 eV) bonds. This inference is consistent with literature reports.[31] The number of oxygen groups is affected by oxidation time. As indicated by Figure 3f, with increasing oxidation time, the amount of hydroxyl and carbonyl groups is found to increase; the amount of carboxyl groups is found to increase to a greater extent than the hydroxyl and carbonyl groups.

With the oxygen-containing carboxyl, carbonyl and hydroxyl groups, the O-MWNT tubes are good hydrogen bond donors/acceptors. The disaccharide head of HDMA behaves as a hydrogen bond acceptor/donor for the functional groups. When in contact with O-MWNT, HDMA molecules can have a hydrogen bonding interaction with the O-MWNT. A longer oxidation time results in more functional groups being generated on the MWNTs (Figure 3f). This facilitates the formation of more hydrogen bonds between O-MWNT and HDMA. As a result, more O-MWNTs can be suspended in the upper organic phase (Figure 1b).

Figure 4 schematically illustrates the hydrogen bonding interactions between the disaccharide group of HDMA and the functional groups of the O-MWNT. The formation of intermolecular hydrogen bonds takes advantage of the structure of the HDMA molecule. It has seven hydroxyl groups, two ether oxygens, one glycosidic oxygen and one N-H. These groups and oxygen atoms can form extensive hydrogen bonds with the functional groups on O-MWNTs. On the other hand, the disaccharide head of HDMA, a maltose structure, presents a sharp bend at the glycosidic bond. This configuration may make the two D-glucopyranose units adapt to the surface of CNTs and favor the formation of hydrogen bonds with the functional groups on the surface of CNTs.

For comparison, nonionic surfactants including Triton X-100, polyvinylpyrrolidone (PVP) and Tween 20 have been used for the phase transfer. They can have hydrogen bonding interactions with substances such as nifedipine,[32] poly(acrylic acid),[33] and parachlorometaxylenol,[34] respectively. PVP and Triton X-100 can only act as hydrogen bond acceptors via the carbonyl oxygen and the ether oxygens. When interacting with Triton X-100 and PVP, the hydroxyl groups and carboxylic acid groups on O-MWNTs can act as hydrogen bond donors. However, some carboxylic acid groups of the O-MWNTs dissociate into H+ cations and COO- anions in the aqueous solution leading to the presence of a net negative charge on the surface of O-MWNTs.[35] As a result, the amount of hydrogen bonds between the surfactants and O-MWNTs is limited. Consequently, Triton X-100 and PVP cannot transfer O-MWNTs into the organic phase (Figure 5). In the case of Tween 20, there are 22 ether oxygens and one carbonyl oxygen, which can act hydrogen bond acceptors. In addition, there are three free terminal hydroxyl groups, which can act both as hydrogen bond acceptors and as donors. Hence, this surfactant can form more hydrogen bonds with O-MWNTs. However, as Tween 20 has much more H-bond acceptors than donors, it cannot form extensive hydrogen bonds with O-MWNTs. As a result, Tween 20 can transfer only a limited number of nanotubes into the organic phase (Figure 5). In the case of ionic surfactants, the cationic surfactant CTAB can transfer some nanotubes into the organic phase, whereas the anionic surfactant AOT cannot (Figure 5). This supports the existence of COO- anions which are attributed to partial dissociation of O-MWNT carboxylic acid groups.[35]

The thermogravimetric analysis (Figure S1) suggests the existence of HDMA molecules in the organic phase. In addition to the HDMA molecules which are hydrogen-bonded to O-MWNTs, some HDMA molecules are self-assembled around O-MWNT. This self-assembly is driven by the chain-chain and hydrogen bonding interactions between HDMA molecules. The dried sample of an upper organic phase was characterized with the X-ray diffraction pattern (Figure S2). As can be seen, the XRD pattern of HDMA (blue) shows two prominent peaks at 19.1° and 23.8°. When interacted with the CNTs, the HDMA shows a prominent peak at 21.3° (olive). It indicates that the symmetry of the crystal structure of HDMA increases after it's self-assembly around O-MWNT. This is probably due to the interactions between the HDMA molecules and O-MWNT, which induced the conformational change of HDMA upon the self-assembly around the MWNTs. As HDMA can dissolve in the organic phase, the self-assembly of HDMA around O-MWNT contributes to

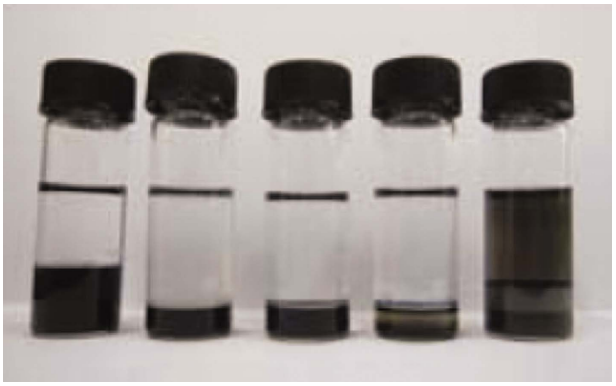

Figure 5. Phase transfer of O-MWNTs with surfactants.

Left to right: Tween 20, Triton X-100, PVP, AOT, CTAB. [Color figure can be viewed in the online issue, which is available at wileyonlinelibrary.com.]

the transfer of O-MWNTs from the aqueous phase to the organic phase.

The self-assembled HDMA showed the ability to "trap" water molecules.[24] Attenuated total reflectance Fourier transform infrared (ATR-FTIR) spectroscopy has been used to monitor the presence of water in an organic phase after phase transfer. Figure 6 shows the ATR-FTIR spectra of the two upper organic phases, into which O-MWNTs were transferred from H_2O and D_2O phases. In the spectrum (blue), the peak at 3,200 cm^{-1} is due to the O-H bond stretching of H_2O. In the spectrum (red), the peak at 2,476 cm^{-1} is assigned to the O—D bond stretching of D_2O. These FTIR spectra indicate that H_2O/D_2O molecules exist in the upper organic phases OP1/OP2 after the phase transfers of CNTs. The presence of water molecules may facilitate the interactions of salt ions with HDMA and O-MWNTs in the organic phase. Solutions of sodium chloride with varying concentrations were added to the organic phase. At a low concentration of 0.05 mol/L, the MWNTs stayed in the organic phase (Figure 7); at a moderate concentration (0.2 mol/L), some O-MWNTs settled at the interface; while at a high concentration (1.0 mol/L), all O-MWNTs were reverted back to the aqueous phase. Sodium ions have shown their interactions with sugars,[36] carbohydrates,[37] and carbonyl groups.[38] The resulting phenomena (Figure 7) may be due to the sodium ion interactions with both HDMA and O-MWNTs. At the low concentration of NaCl (0.05 mol/L), the sodium ions might interact with some sugar head groups of HDMA, but they might not interact with functional groups of O-MWNTs and the sugar head groups in contact with the MWNTs. As a result, the hydrogen bonds formed between the HDMA and O-MWNTs are reserved. While at the high concentration of sodium chloride (1.0 mol/L), sodium ions might have a higher chance of interacting with the functional groups and the sugar head groups in contact with the O-MWNTs. The hydrogen bonding interactions between the sugar groups and the functional groups might, thus, be greatly reduced. This results in the MWNTs falling back to the aqueous phase. Therefore, aqueous solutions of sodium chloride can be used to regulate the phase transfer of CNTs.

According to the principle of the hydrogen bonding interactions between the disaccharide group of HDMA and the functional groups of O-MWNTs, HDMA was used to transfer the carbon nanotubes, which were functionalized with amino-cyclodextrin, as schematically presented in Figure S3.

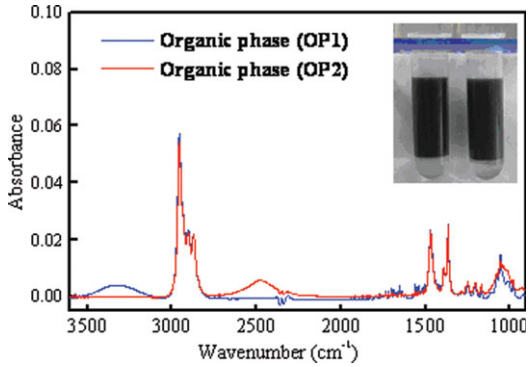

Figure 6. FTIR spectra of the upper organic phases.

OP1 (blue): the aqueous phase is H_2O. OP2 (Red): the aqueous phase is D_2O. The insert showing O-MWNTs in OP1 and OP2. [Color figure can be viewed in the online issue, which is available at wileyonlinelibrary.com.]

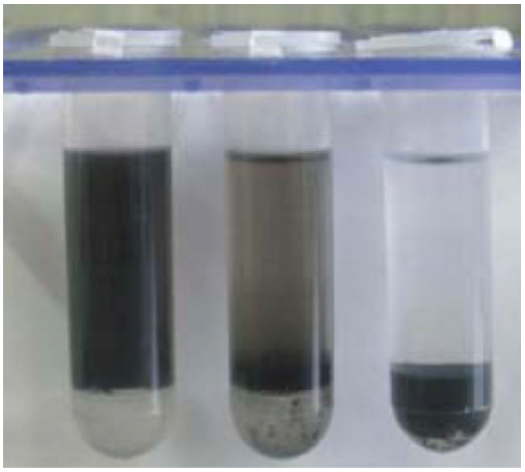

Figure 7. Effect of NaCl solution on the phase transfer.

Left to right (NaCl concentration, mol/L): 0.05, 0.2, 1.0. [Color figure can be viewed in the online issue, which is available at wileyonlinelibrary.com.]

For the synthesis of the amino-cyclodextrin and the functionalization of MWNTs (refer to our previous work).[39] As seen in Figure S4, the functionalized MWNTs (f-MWNTs) can be transferred from the aqueous phase to the organic phase. This transfer uses the hydrogen bonding interactions between the disaccharide group of HDMA and the cyclodextrin motif on f-MWNTs. The HRTEM (Figure S4b) shows that HDMA molecules are assembled on the MWNT. In addition, for phase transfers of O-MWNTs and f-MWNTs, carbon tetrachloride and mixtures of hexane/isopropyl alcohol and petroleum ether/n-butanol can be used as organic solvents/phases.

Conclusions

We have demonstrated that oxidized MWNTs can be transferred from the aqueous phase to the organic phases with HDMA. The phase transfer uses the hydrogen bonds formed between the head groups of HDMA and the oxygen groups on O-MWNTs. This principle has been extended to the phase transfer of amino-cyclodextrin functionalized MWNTs. With the methodology, the dissolutions of O-MWNTs and f-MWNTs in a wide range of organic solvents are enabled, including isooctane/n-propanol, carbon tetrachloride, hexane/isopropyl alcohol, and petroleum ether/n-butanol.

Acknowledgments

The authors acknowledge the National Science Foundation of China (21076018, 21176025).

Literature Cited

1. Cherukuri P, Bachilo SM, Litovsky SH, Weisman RB. Near-infrared fluorescence microscopy of single-walled carbon nanotubes in phagocytic cells. *J Am Chem Soc*. 2004;126:15638–15639.
2. Ovejero G, Sotelo JL, Romero MD, Rodrıguez A, Ocan MA, Rodrıguez G, Garcıa J. Multiwalled carbon nanotubes for liquid-phase oxidation. functionalization, characterization, and catalytic activity. *Ind Eng Chem Res*. 2006;45:2206–2212.
3. Liu XY, O'Carroll DM, Petersen EJ, Huang QG, Anderson CL. Mobility of multiwalled carbon nanotubes in porous media. *Environ Sci Technol*. 2009;43:8153–8158.
4. Kim KT, Edgington AJ, Klaine SJ, Cho JW, Kim SD. Influence of multiwalled carbon nanotubes dispersed in natural organic matter on speciation and bioavailability of copper. *Environ Sci Technol*. 2009;43:8979–8984.

5. Simon-Deckers A, Loo S, Mayne-L'hermite M, Herlin-Boime N, Menguy N, Reynaud C, Gouget B, Carriere M. Size-, composition- and shape-dependent toxicological impact of metal oxide nanoparticles and carbon nanotubes toward bacteria. *Environ Sci Technol*. 2009;43:8423–8429.
6. Yan X, Han Z, Yang Y, Tay B. Fabrication of carbon nanotube–polyaniline composites via electrostatic adsorption in aqueous colloids. *J Phys Chem C*. 2007;111:4125–4131.
7. Ballesteros B, de la Torre G, Ehli C, Rahman GMA, Agullo-Rueda F, Guldi DM, Torres T. Single-wall carbon nanotubes bearing covalently linked phthalocyanines photoinduced electron transfer. *J Am Chem Soc*. 2007;129:5061–5068.16.
8. Yao Z, Braidy N, Botton GA, Adronov A. Polymerization from the surface of single-walled carbon nanotubes preparation and characterization of nanocomposites. *J Am Chem Soc*. 2003;125: 16015–16024.
9. Chen J, Hamon MA, Hu H, Chen Y, Rao AM, Eklund PC, Haddon RC. Solution. Properties of single-walled carbon nanotubes. *Science*. 1998;282:95–98.
10. Hamon MA, Chen J, Hu H, Chen Y, Rao AM, Eklund PC, Haddon RC. Dissolution of single-walled carbon nanotubes. *Adv Mater*. 1999;11:834–840.
11. Chen J, Rao AM, Lyuksyutov S, Itkis ME, Hamon MA, Hu H, Cohn RW, Eklund PW, Colbert DT, Smalley RE, Haddon RC. Dissolution of full-length single-walled carbon nanotubes. *J Phys Chem B*. 2001;105:2525–2528.
12. Hu H, Zhao B, Hamon MA, Kamaras K, Itkis ME, Haddon RC. Sidewall functionalization of single-walled carbon nanotubes by addition of dichlorocarbene. *J Am Chem Soc*. 2003;125:14893–14900.
13. Bahr JL, Yang J, Kosynkin DV, Bronikowski MJ, Smalley RE, Tour JM. Functionalization of carbon nanotubes by electrochemical reduction of aryl diazonium salts: a bucky paper electrode. *J Am Chem Soc*. 2001;123:6536–6542.
14. Deria P, Sinks LE, Park TH, Tomezsko DM, Brukman MJ, Bonnell DA, Therien MJ. Phase transfer catalysts drive diverse organic solvent solubility of single-walled carbon nanotubes helically wrapped by ionic, semiconducting polymers. *Nano Lett*. 2010;10:4192–4199.
15. Ziegler KJ, Schmidt DJ, Rauwald U, Shah KN, Flor EL, Hauge RH, Smalley RE. Length-dependent extraction of single-walled carbon nanotubes. *Nano Lett*. 2005;5:2355–2359.
16. Kakade B, Patil S, Sathe B, Gokhale S, Pillai V. Mercurycyclopentadienyl derivatives are not always fluxional. *J Am Chem Soc*. 2008;120:599–600.
17. Gao J, Itkis ME, Yu A, Bekyarova E, Zhao B, Haddon RC. Continuous spinning of a single-walled carbon nanotube–nylon composite fiber. *J Am Chem Soc*. 2005;127:3847–3854.
18. Shi Y, Fu D, Marsh DH, Rance GA, Khlobystov AN, Li LJ. Photoresponse in self-assembled films of carbon nanotubes. *J Phys Chem C*. 2008;112:13004–13009.
19. Lee KY, Kim M, Hahn J, Suh JS, Lee I, Kim K, Han SW. Assembly of metal nanoparticle–carbon nanotube composite materials at the liquid/liquid interface. *Langmuir*. 2006;22:1817–1821.
20. Asuri P, Karajanagi SS, Dordick JS, Kane RS. Directed assembly of carbon nanotubes at liquid–liquid interfaces: nanoscale conveyors for interfacial biocatalysis. *J Am Chem Soc*. 2006;128:1046–1047.
21. Yi H, Song H, Chen X. Carbon nanotube capsules self-assembled by w/o emulsion technique. *Langmuir*. 2007;23:3199–3204.
22. Wang RK, Reeves RD, Ziegler KJ. Interfacial trapping of single-walled carbon nanotube bundles. *J Am Chem Soc*. 2007;129:15124–15125.
23. Wang RK, Park HO, Chen WC, Batista C S, Reeves RD, Butler JE, Ziegler KJ. Improving the effectiveness of interfacial trapping in removing single-walled carbon nanotube bundles. *J Am Chem Soc*. 2008;130:14721–14728.
24. Bhattacharya S, Acharya SNG. Pronounced hydrogel formation by the self-assembled aggregates of n-alkyl disaccharide amphiphiles. *Chem Mater*. 1999;11:3504–3511.
25. Liu J, Rinzler AG, Dai H, Hafner JH, Bradley RK, Boul PJ, Lu A, Iverson T, Shelimov K, Huffman CB, Rodriguez-Macias F, Shon YS, Lee TR, Colbert DT, Smalley RE. Fullerene pipes. *Science*. 1998;280:1253–1254.
26. Parry KL, Shard AG, Short RD, White RG, Whittle JD, Wright A. ARXPS characterisation of plasma polymerised surface chemical gradients. *Surf Interface Anal*. 2006;38:1497–1504.
27. Shirley DA. High-resolution x-ray photoemission spectrum of the valence bands of gold. *Phys Rev B*. 1972;5:4709–4714.
28. Stevens JS, Schroeder SL. M. Quantitative analysis of saccharides by X-ray photoelectron spectroscopy. *Surf Interface Anal*. 2009;41:453–462.
29. Banerjee S, Wong SS. Synthesis and characterization of carbon nanotube–nanocrystal heterostructures. *Nano Lett*. 2002;2:195–200.
30. Mawhinney DB, Naumenko V, Kuznetsova A, Yates J T, Jr. Infrared spectral evidence for the etching of carbon nanotubes: ozone oxidation at 298 K. *J Am Chem Soc*. 2000;122:2383–2384.
31. Kovtyukhova NI, Mallouk TE, Pan L, Dickey EC. Individual single-walled nanotubes and hydrogels made by oxidative exfoliation of carbon nanotube ropes. *J Am Chem Soc*. 2003;125:9761–9769.
32. Rumondor ACF, Marsac PJ, Stanford LA, Taylor LS. Phase behavior of poly(vinylpyrrolidone) containing amorphous solid dispersions in the presence of moisture. *Mol Pharm*. 2009;6:1492–1505.
33. Galatanu A N, Chronakis I S, Anghel DF, Khan A. Ternary phase diagram of the triton x-100/poly(acrylic acid)/water system. *Langmuir*. 2000;16:4922–4928.
34. Breuninger WB, Goettsch RW. Interaction of parachlorometaxylenol with macromolecules. *J Pharm Sci*. 1965;54:1487–1490.
35. Jaber-Ansari L, Hahm MG, Somu S, Sanz YE, Busnaina A, Jung Y J. Mechanism of very large scale assembly of SWNTs in template guided fluidic assembly process. *J Am Chem Soc*. 2009;131: 804–808.
36. Detellier C, Grandjean J, Laszlo P. Interactions of sugars with the sodium cation. Sensitivity of the sodium-23 nuclear magnetic resonance line width in pyridine solution. *J Am Chem Soc*. 1976; 98:3375–3376.
37. Angyai SJ. Complexing of polyols with cations. *Tetrahedron*. 1974;30:1695–1702.
38. Douhal A, Roshal AD, Organero JA. Stepwise interactions, sodium ion photoejection and proton-transfer inhibition in a crown-ether and proton-transfer dye. *Chem Phys Lett*. 2003;381:519–525.
39. Li L, Feng W, Ji P. Protein adsorption on functionalized multiwalled carbon nanotubes with amino-cyclodextrin. *AIChE J*. 2011;57:3507–3513.

Manuscript received Nov. 9, 2011, and revision received Dec. 21, 2011.